Effect of Reinforcing Carbon Black on Network Structure, Technical Properties, and Failure Mode of EPDM Rubber

PRANAB K. PAL and S. K. DE, *Rubber Technology Centre, Indian Institute of Technology, Kharagpur 721302, India*

Synopsis

The high sulfur (HS) vulcanization system gives rise to higher apparent crosslink density and improvement in modulus, resistance to abrasion, compression set, heat buildup, rebound resilience, and dynamic set than that of the low sulfur (LS) vulcanization system. Tensile strength, tear strength, and flexing resistance were found to be better for the low sulfur (LS) vulcanization system. Rupture energy during tensile and tear failure determined from the Universal Testing Machine (Instron 1195) also reveals a similar phenomenon. Studies on fracture mode during different types of failure have been done by using a scanning electron microscope (SEM).

INTRODUCTION

Reinforcement of an elastomer means improvement of failure properties like tensile, tear, abrasion, and flexing. Reinforcement can be achieved by incorporation of fine particulate fillers like carbon blacks. In previous papers,[1-5] we have reported changes in network structure, technical properties, and failure mode of natural rubber (NR) on addition of carbon black. Correlation between nature of failed or damaged zone and different physical properties has been analyzed. Such studies have been found to be useful in understanding the strength and failure of rubbers.

In this present paper, we report results of our studies on the effect of increasing addition of reinforcing carbon black (ISAF, N 220) on network structure, technical properties, and failure of EPDM rubber vulcanizates. Two vulcanizing systems, high sulfur (HS) and low sulfur (LS) systems, have been chosen. Analyses of failure surfaces have been done by SEM.

EXPERIMENTAL

The formulations of the mixes are shown in Table I. Their curing parameters as obtained from Monsanto rheometer (R-100) at 150°C are shown in Table II. The mixes were prepared on a conventional laboratory size rubber mill (32.5 cm × 15 cm). Vulcanization was carried out at 150°C in an electrically heated press. Moldings were immersed in water for cooling immediately after the end of the curing cycle.[6]

Determination of Polymer–Filler Interaction. Polymer–filler interaction

Journal of Applied Polymer Science, Vol. 28, 3333–3347 (1983)

CCC 0021-8995/83/113333-15$02.50

TABLE I
Formulations of Mixes

	Mix							
	A	B	C	D	E	F	G	H
Nordel 2722[a]	100	100	100	100	100	100	100	100
Zinc oxide	5	5	5	5	5	5	5	5
Stearic acid	1	1	1	1	1	1	1	1
ISAF black (N 220)[b]	—	5	25	50	—	5	25	50
Naphthenic oil	—	1	5	10	—	1	5	10
MBT[c]	1.5	1.5	1.5	1.5	1	1	1	1
TMTD[d]	2	2	2	2	3	3	3	3
Sulfur	2	2	2	2	0.5	0.5	0.5	0.5

[a] High ethylene content ethylene–propylene–1,4-hexadiene terpolymer, obtained from Indian Cable Company Ltd., Jamshedpur, India.

[b] Intermediate superabrasion furnace black, obtained from Phillips Carbon Black Ltd., Durgapur, India.

[c] Mercaptobenzothiazole, obtained from Alkali and Chemical Corp. of India Ltd., Rishra.

[d] Tetramethylthiuram disulfide, obtained from Alkali and Chemical Corp. of India Ltd., Rishra.

was determined using the following equation of Cunneen and Russell[7] [eq. (3)], which is the modified equation of Lorenz and Parks[8] [eq. (1)]:

$$\frac{Q_f}{Q_g} = ae^{-Z} + b \tag{1}$$

and also

$$\frac{Q_f}{Q_g} = \frac{V_{r0}(1 - V_{rf})}{V_{rf}(1 - V_{r0})} \simeq \frac{V_{r0}}{V_{rf}} \tag{2}$$

so that

$$\frac{V_{r0}}{V_{rf}} = ae^{-Z} + b \tag{3}$$

where Q is the amount of solvent imbibed per unit weight of the rubber, f and g refer to filled and gum mixes, V_{r0} and V_{rf} are the volume fractions of rubber in unfilled and filled vulcanizates, respectively, swollen in a solvent, Z is the weight fraction of filler in the vulcanizate, and a and b are constants characteristic of the system. Polymer–filler interaction was also studied by using the following equation of Kraus[9]:

$$V_{r0}/V_{rf} = 1 - m\phi/(1 - \phi) \tag{4}$$

where

$$m = 3c(1 - V_{r0}^{1/3}) + V_{r0} - 1 \tag{5}$$

Here ϕ is the volume fraction of filler in the filled vulcanizate and c is a constant characteristic of the filler, but independent of the polymer, the solvent, or the degree of vulcanization.

Determination of Network Structure and Technical Properties. The volume fraction of rubber (V_r) in the vulcanizates swollen in a solvent, sulfur-

TABLE II
Curing Characteristics of Mixes at 150°C

	High sulfur (HS) system				Low sulfur (LS) system			
ISAF black (phr)	0	5	25	50	0	5	25	50
Mix	A	B	C	D	E	F	G	H
Rheometric scorch time t_2 (min)	5.5	5.0	3.5	3.5	9.0	8.0	6.0	6.0
Rheometric optimum cure time (min)	23.5	23.0	18.5	20.5	40.0	36.0	26.0	25.5

combined [Sc] in the network, free sulfur, sulfide sulfur [S^{-2}] concentrations, and technical properties of the vulcanizates were determined by the methods as adopted in our previous studies.[1,6]

The "apparent" chemical crosslink density was determined[10] by swelling of a weighed sample of vulcanizate in benzene till the equilibrium swelling was attained, which was 8 h in this case. The swelling value Q (g benzene/g rubber hydrocarbon) was calculated from the equation of Parks and Brown[11] as follows:

$$Q = \frac{\text{(swollen wt} - \text{dried wt)}}{\text{(original wt} \times 100/\text{formula wt)}} \tag{6}$$

where formula weight is the total weight of rubber plus compounding ingredients based on 100 parts of rubber. A comparison of the crosslinking was then made from the reciprocal swelling value, $1/Q$.

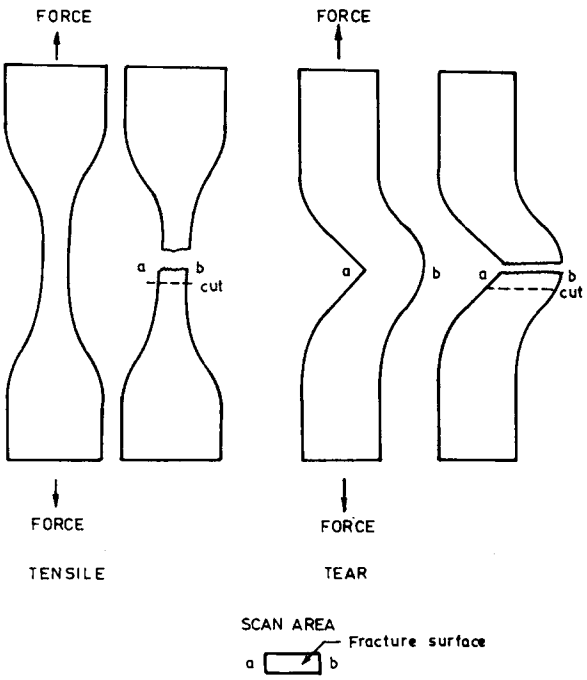

Fig. 1. Mode of failure after tension and tear and scan area of fracture surface.

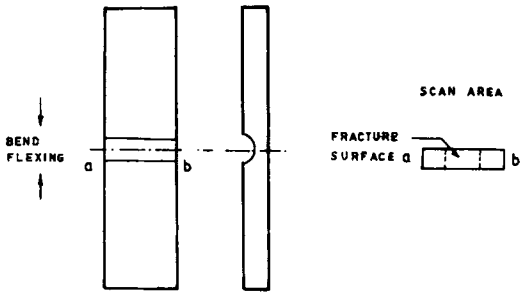

Fig. 2. Mode of failure after bend flexing and scan area of fracture surface.

The sulfur inefficiency parameter [E_m], which is the number of sulfur atoms combined in the network per chemical crosslink, is defined here as[12]

$$[E_m] = \frac{[Sc]}{V_r} \tag{7}$$

since the calculation of "true" chemical crosslink density is less certain for filled EPDM rubber vulcanizates.

Scanning Electron Microscopy Studies. Figure 1 shows the direction in which stress was applied in tension and tear tests. Figure 2 shows the direction in which bend flexing occurs. After the completion of tensile, tear, and flexing tests, the fracture surfaces were carefully cut out from one of the two pieces of the failed test specimens without touching the surface.

The fractured test specimens were stored in a desiccator in order to avoid contamination and then sputter-coated with gold within 24 h of testing. SEM photomicrographs of the tested specimens were taken using the Phillips 500 scanning electron microscope at 0° tilt. The respective scan areas of the specimens are also shown in Figures 1 and 2.

Determination of Rupture Energy. Rupture energy during tensile and tear failure was determined using the Universal Testing Machine (Instron 1195) by the following formula,

$$E = \frac{K \times L \times S}{10{,}000}$$

where E = rupture energy (kg·mm), L = full scale load (kg), S = rate of sample extension (crosshead speed) (mm/min), K = integrator reading.

RESULTS AND DISCUSSION

Curing Characteristics

It is evident from Table II that rheometric scorch time of the low sulfur (LS) system is higher than that of the high sulfur (HS) system and addition of carbon black reduces the scorch time in both cases. Optimum cure time (o.c.t.) of the LS system is higher than that of the HS system. Addition of carbon black reduces the o.c.t. in both cases, but the reduction is drastic in the LS system and only marginal in the HS system. Our earlier work[1] with natural rubber also showed a similar type of phenomenon.

TABLE III
Chemical Characterization of Vulcanizates[a]

	HS system				LS system			
ISAF black (phr)	0	5	25	50	0	5	25	50
Mix	A	B	C	D	E	F	G	H
Volume fraction of rubber V_r	0.363	0.366	0.374	0.390	0.303	0.306	0.309	0.322
Apparent crosslink density $1/Q$	0.555	0.562	0.575	0.612	0.439	0.443	0.447	0.469
Apparent polysulfidic crosslinks	0.265 (48)	0.268 (48)	0.275 (48)	0.283 (46)	0.152 (35)	0.153 (35)	0.177 (40)	0.191 (41)
Network combined sulfur [Sc] (g/100 g RH)	1.429	1.429	1.435	1.513	0.189	0.238	0.257	0.302
Sulfur inefficiency parameter, E_s (g/100 g RH)	3.9	3.9	3.8	3.9	0.6	0.8	0.8	0.9
Free sulfur concentration (mmol/kg RH)	174	174	171	149	97	82	76	62
Sulfide sulfur [S^{-2}] concentration (mmol/kg RH)	4.4	4.6	5.6	3.4	b	b	b	b

[a] Values in parentheses are percentage of apparent polysulfidic crosslinks.
[b] Values are negligible.

TABLE IV
Physical Properties of Vulcanizates[a]

	HS system				LS system			
ISAF black (phr)	0	5	25	50	0	5	25	50
Mix	A	B	C	D	E	F	G	H
Modulus 300% (MPa)	2.9 (—)	3.9 (—)	8.6 (—)	15.6 (—)	2.4 (120)	2.8 (142)	6.1 (231)	11.0 (220)
Tensile strength (MPa)	3.8 (72)	7.4 (65)	20.5 (62)	22.8 (91)	4.8 (67)	9.3 (59)	22.9 (69)	23.4 (98)
Elongation at break (%)	350 (72)	425 (54)	460 (46)	390 (45)	500 (66)	560 (62)	600 (55)	540 (51)
Tear strength ($kN \cdot m^{-1}$)	14.3 (65)	18.2 (66)	34.8 (58)	43.2 (56)	18.1 (86)	26.2 (71)	40.9 (66)	47.5 (72)
Hardness (shore A)	83 (97)	84 (97)	87 (100)	93 (100)	82 (98)	83 (98)	86 (100)	91 (101)
Compression set (%)	8	8	9	11	12	13	15	16
Abrasion loss (cc/1000 rev)	5.8	1.8	0.5	0.2	8.0	2.3	0.7	0.4
Flex cracking resistance (k cycles)	0.2	0.2	35	26	0.2	0.4	51	42
Heat buildup ΔT (°C)	11	12	22	30	19	23	33	43
Rebound resilience (%)	54	51	48	44	51	50	44	39
Dynamic set (%)	1.1	1.3	1.7	2.8	2.0	2.2	3.5	5.1

[a] Values in parentheses are % retained of respective properties after aging at 100°C for 4 days.

TABLE V
Rupture Energy Obtained Using Universal Testing Machine (Instron 1195)

	HS system		LS system	
ISAF block (phr)	5	50	5	50
Mix	B	D	F	H
Rupture energy for tensile failure (kg·mm × 10^{-2})	33.9	111.4	49.1	122.7
Rupture energy for tear failure (kg·mm × 10^{-2})	10.2	19.7	12.5	27.0

Network Structure

Analyses of Table III showed that apparent crosslink density (as measured by volume fraction of rubbber, V_r, in the swollen vulcanizate) is higher in the HS system and addition of ISAF black only marginally increases V_r at higher filler loading (50 phr). In the presence of black, concentration of polysulfidic crosslinks is not affected in the HS-system (46–48%), but in the case of the LS system polysulfidic crosslinks increase marginally from 35% to 41% on addition of 50 phr ISAF black. As expected, network-combined sulfur [Sc] and free sulfur are less in the LS system. Increasing addition of ISAF black increases the [Sc] and reduces the free sulfur, indicating formation of higher amount of sulfurating complexes at higher filler loading. This, in turn, increases the V_r values at higher filler loading. The sulfur inefficiency parameter [E_m] in the LS system is less than that of the HS system, showing that sulfur is more efficiently utilized in the former system.

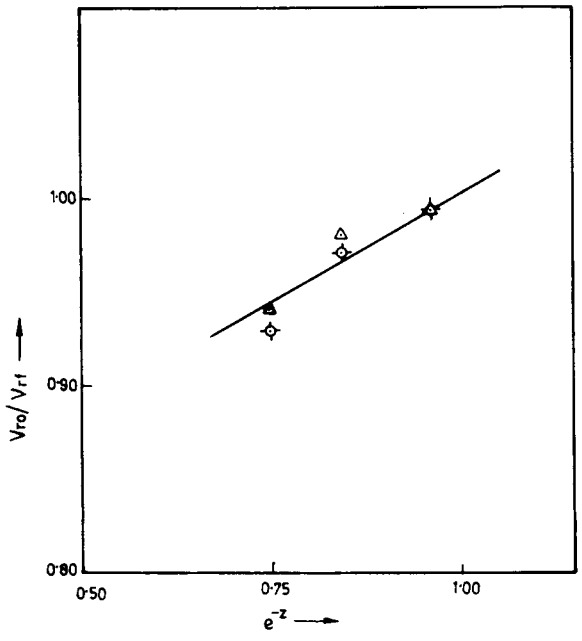

Fig. 3. Plot of V_{r0}/V_{rf} against e^{-z} for high sulfur (⊙) and low sulfur (△) systems.

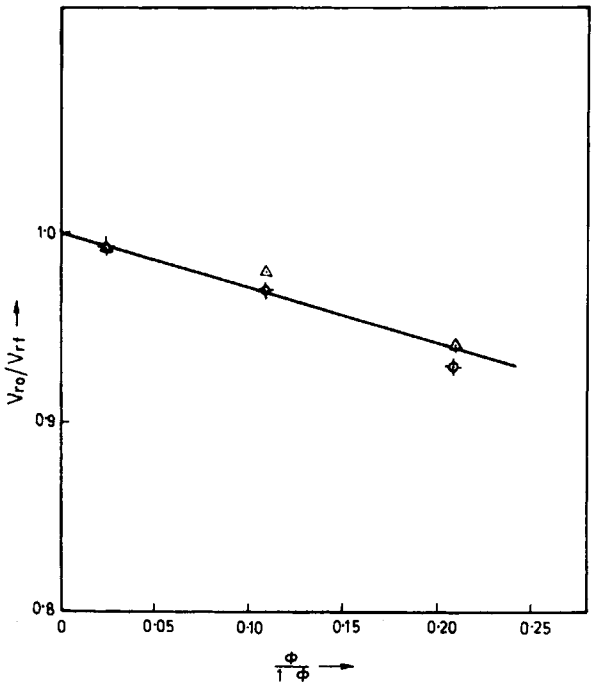

Fig. 4. Plot of V_{r0}/V_{rf} against $\phi/(1-\phi)$ for high sulfur (⊙) and low sulfur (△) systems.

TECHNICAL PROPERTIES

Technical properties, as summarized in Table IV, show that:

1. Modulus and hardness of the HS system are higher than that of the LS system, possibly due to higher V_r in the former case, and, as expected, addition of ISAF black increases the modulus and hardness in all cases.

2. The HS system shows lower compression set, lower heat buildup, lower dynamic set, and higher resilience than the LS system at all filler loadings. This behavior can be ascribed to a lower degree of crosslinking in the LS system. Expectedly, incorporation of filler increases the set and heat buildup due to high hysteresis loss.

3. EPDM rubber, unlike natural rubber, is not self-reinforcing, and reinforcing filler is essential for development of strength. This is apparent in the tensile, tear, flex cracking, and abrasion resistance. Tensile and tear properties of the LS system are slightly higher than those of the HS system. This is also evident from the higher rupture energy (Table V) of the vulcanizates. Lower V_r values may be responsible for the higher flex crack resistance of the LS system. Abrasion loss of the LS system is higher than that of the HS system; this seems to be due to lower degree of crosslinking in the former case.

Plot of V_{r0}/V_{rf} vs. e^{-Z} (Fig. 3) shows that both the LS- and HS-systems show similar extent of polymer–filler interaction. This is also evident in the Kraus plots (Fig. 4). Therefore, variation in the physical properties (Table IV) are to be assigned to the changes in the network structures of the two systems (Table III) and not to the polymer–filler interaction. Further insight into this problem

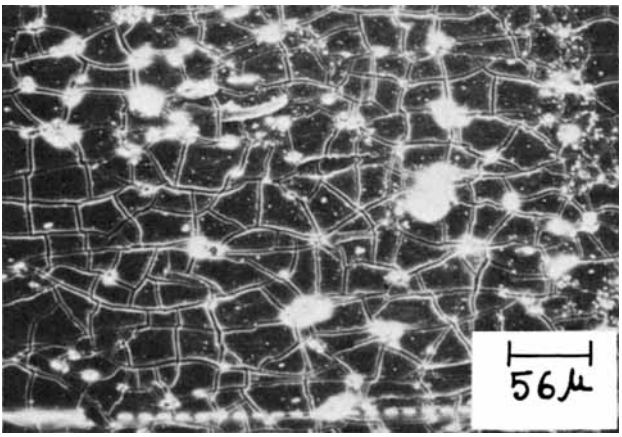

Fig. 5. SEM photograph of tensile fracture surface: surface showing channel-type cracks forming a network of mix A.

can be obtained from analyses of the SEM photomicrographs of the fracture surfaces.

Scanning Electron Microscopy Studies

Tensile Fracture Surface. Figures 5 and 6 are the fractographs of gum EPDM rubber vulcanizates of the HS and LS systems. The network of surface cracks is the characteristic feature in both cases. The addition of a lower amount of ISAF black changes the fracture surface. A long and steady tear line, along with cracks, is visible in the HS system (Fig. 7), while shorter tear lines, a rough surface, and a network of cracks are the features of the LS system (Fig. 8). The strength of the LS system is higher than that of the HS system, which is manifested in the roughness of the fracture surface.[13–15] The addition of a higher amount (50 phr) of ISAF black shows an almost similar type of network of cracks in the smooth fracture surface of the HS system (Fig. 9), whereas the LS system shows a rough surface with a relatively lesser extent of cracks (Fig. 10).

Tear Fracture Surface. Gum EPDM vulcanizate has low tear strength. Figure 11 shows a cleavage fracture-forming feathery band in the HS system which is reduced by the addition of 5 phr ISAF black as shown in Figure 13, which shows a fracture surface consisting of flat dimples. An increase in filler loading to 50 phr changes the failure pattern, and the fracture surface (Fig. 15) looks like the tensile fractograph. The LS system shows different characteristics. Figure 12 for gum vulcanizate shows the presence of tear paths and channel-type cracks. The addition of 5 phr ISAF black makes the surface rough, and cracks and tear paths are also observable (Fig. 14). The incorporation of 50 phr ISAF black decreases the sizes of the tear paths (Fig. 16), and instead a large number of smaller tear lines superimposed on the cracks are visible.

Flex Fracture Surface. Figure 17 shows a brittle fracture surface of the high sulfur EPDM vulcanizate containing 5 phr ISAF black, which failed under De Mattia flexing. An increase in filler loading (50 phr) changes the fracture surface, which shows a featherlike fracture band (Fig. 19). The LS system at 5 phr

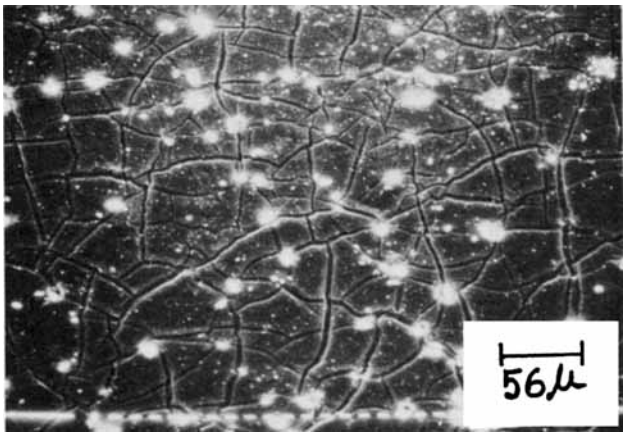

Fig. 6. SEM photograph of tensile fracture surface: surface showing network of channel-type cracks of mix E.

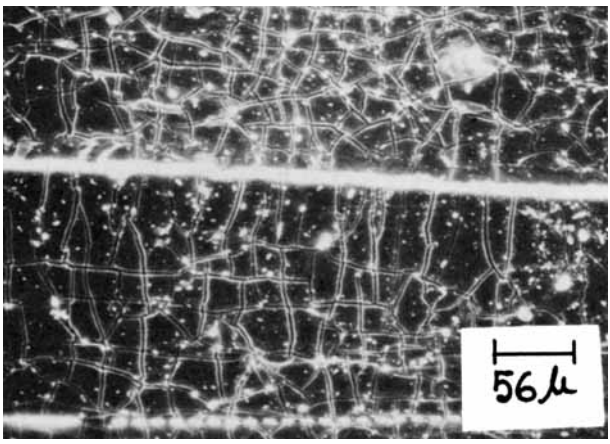

Fig. 7. SEM photograph of tensile fracture surface: steady tear line and the network of cracks of mix B.

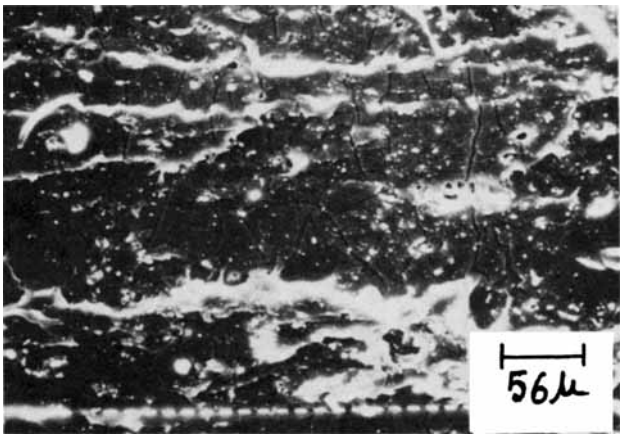

Fig. 8. SEM photograph of tensile fracture surface: shorter tear lines and network of cracks on the rough fracture surface of mix F.

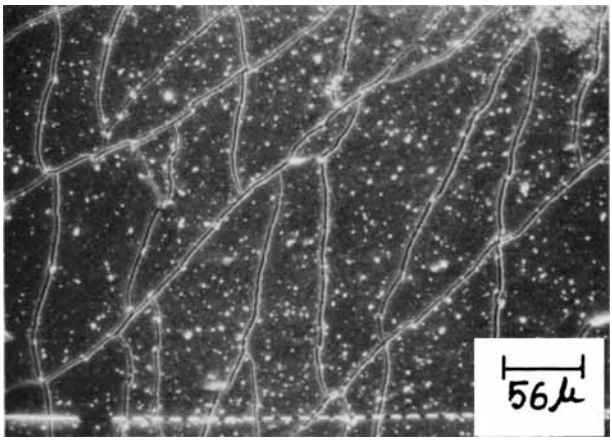

Fig. 9. SEM photograph of tensile fracture surface: long channel-type cracks loosely bound of mix D.

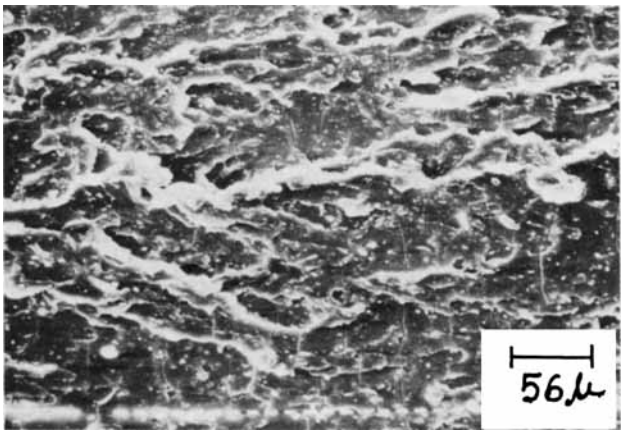

Fig. 10. SEM photograph of tensile fracture surface: rough surface containing nonsteady tear lines and small cracks of mix H.

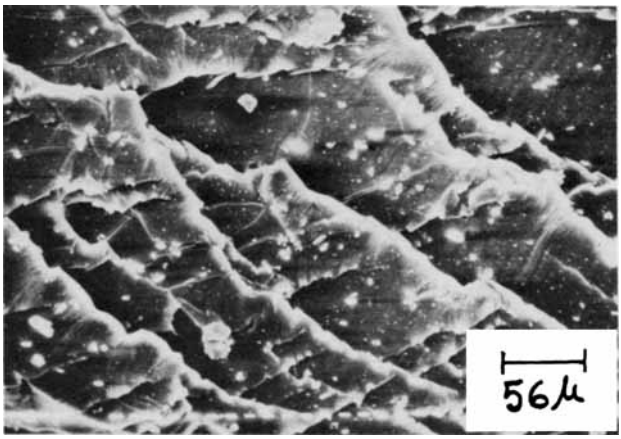

Fig. 11. SEM photograph of tear fracture surface: cleavage fracture forming feathery band of mix A.

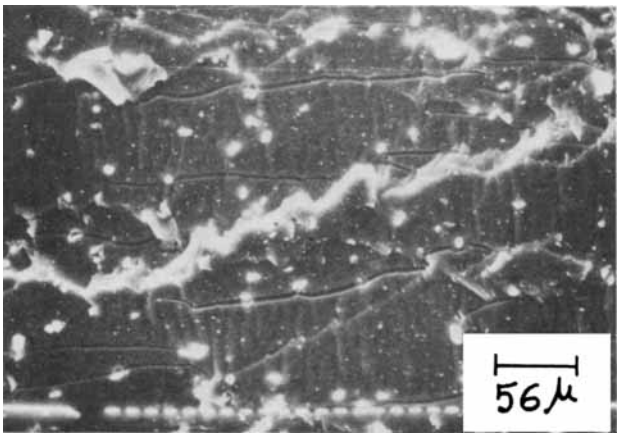

Fig. 12. SEM photograph of tear fracture surface: tear path and parallel channel-type cracks of mix E.

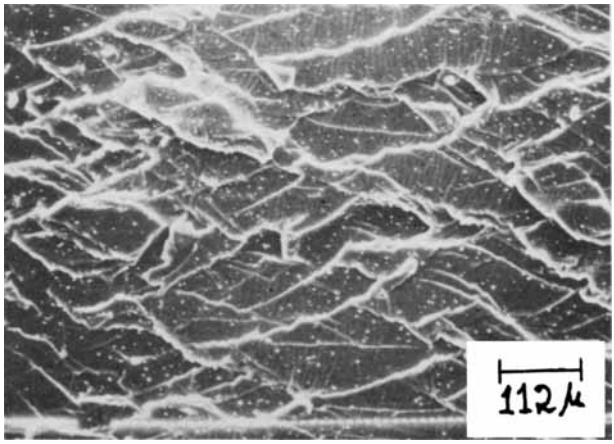

Fig. 13. SEM photograph of tear fracture surface: surface showing flat dimples of mix B.

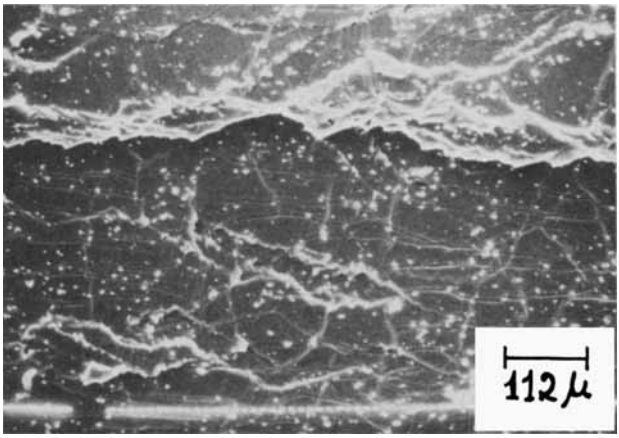

Fig. 14. SEM photograph of tear fracture surface: tear path with straight channel-type cracks of mix F.

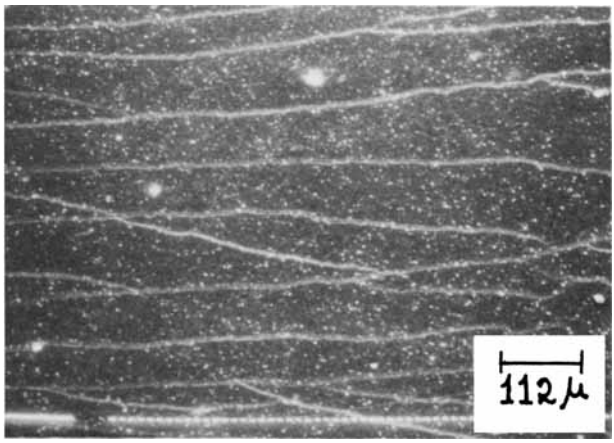

Fig. 15. SEM photograph of tear fracture surface: steady and parallel channel-type cracks on the smooth fracture surface of mix D.

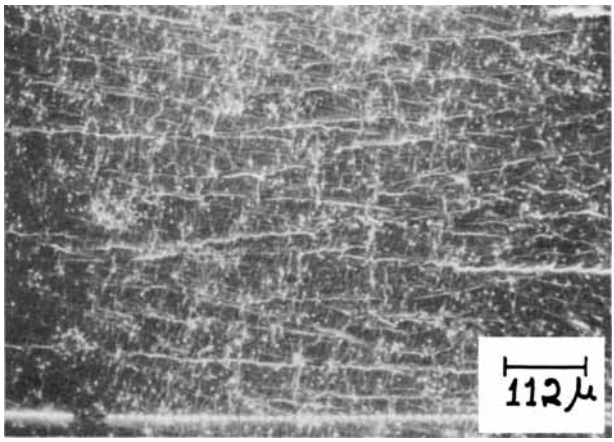

Fig. 16. SEM photograph of tear fracture surface: a large number of smaller tear lines superimposed on the cracks of mix H.

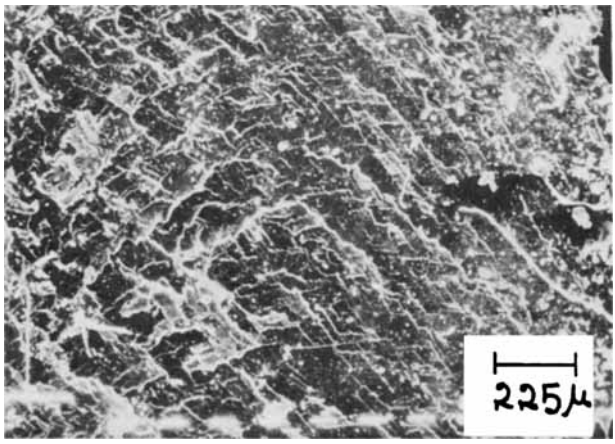

Fig. 17. SEM photograph of flex fracture surface: general surface showing brittle fracture of mix B.

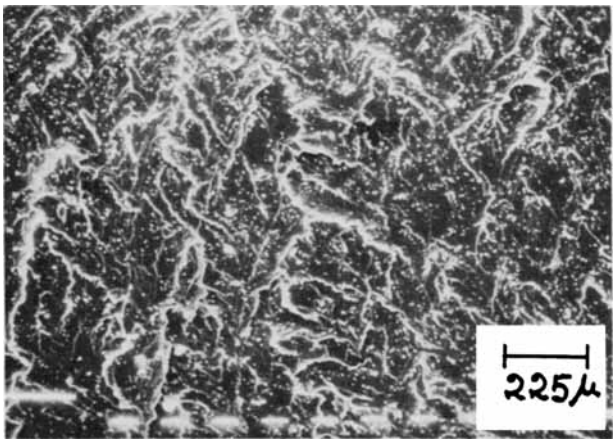

Fig. 18. SEM photograph of flex fracture surface: general surface showing brittle failure of mix F.

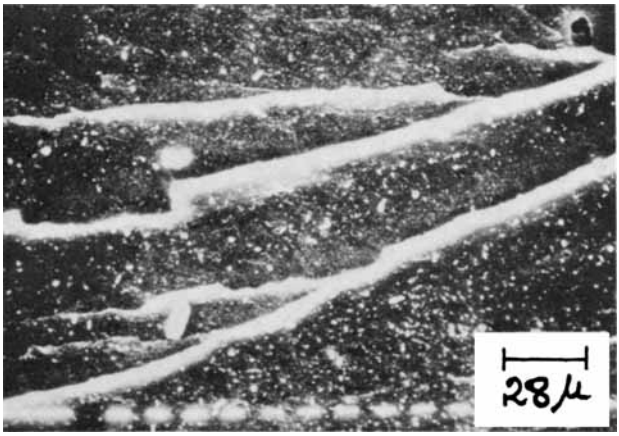

Fig. 19. SEM photograph of flex fracture surface: cleavage fracture forming feathery band of mix D.

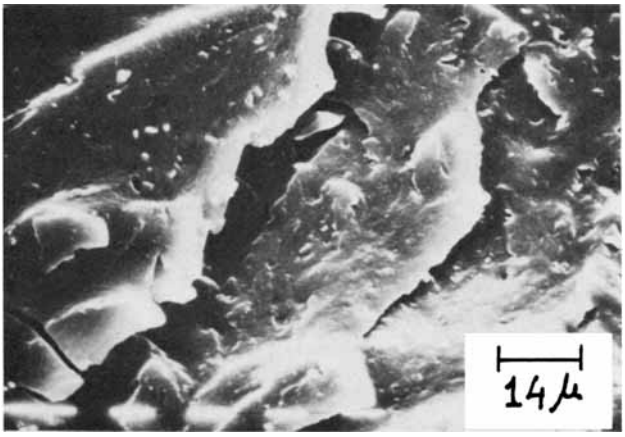

Fig. 20. SEM photograph of flex fracture surface: ductile failure of mix H.

loading shows characteristics (Fig. 18) similar to those of the HS system. But at higher filler loading the LS system shows characteristics different from those of the HS system. No featherlike fracture bands are observable. The failure was of the ductile type with cleavage (Fig. 20). The fatigue strength of the LS vulcanizate at higher filler loading was also found to be higher than that of the HS vulcanizate.

CONCLUSIONS

The HS system produces higher modulus, hardness, rebound resiliance, resistance to abrasion, lower heat buildup, compression set, and dynamic set as compared to the LS system. The tensile strength, tear strength, and resistance to flexing are better in the LS system.

Changes in the strength of the vulcanizates of the HS and LS systems have been correlated with the fractographs obtained by SEM studies of fractured surfaces which failed under tension, tear, and flexing.

References

1. P. K. Pal, A. K. Bhowmick, and S. K. De, *Rubber Chem. Technol.*, **55,** 23 (1982).
2. P. K. Pal, A. K. Bhowmick, and S. K. De, *Int. J. Polym. Mater.*, **9,** 139 (1982).
3. N. M. Mathew, A. K. Bhowmick, B. K. Dhindaw, and S. K. De, *J. Mater. Sci.*, **17,** 2594 (1982).
4. N. M. Mathew and S. K. De, *Polymer*, **23,** 632 (1982).
5. N. M. Mathew, A. K. Bhowmick, and S. K. De, *Rubber Chem. Technol.*, **55,** 51 (1982).
6. R. Mukhopadhyay and S. K. De, *Polymer*, **18,** 1243 (1977).
7. J. I. Cunneen and R. M. Russell, *Rubber Chem. Technol.*, **43,** 1215 (1970).
8. O. Lorenz and C. R. Parks, *J. Polym. Sci.*, **50,** 299 (1961).
9. G. Kraus, *J. Appl. Polym. Sci.*, **7,** 861 (1963); *Rubber Chem. Technol.*, **37,** 6 (1964).
10. R. Mukhopadhyay and S. K. De, *Rubber Chem. Technol.*, **52,** 263 (1979).
11. C. R. Parks and R. J. Brown, *Rubber Chem. Technol.*, **49,** 233 (1976).
12. A. K. Bhowmick and S. K. De, *Rubber Chem. Technol.*, **53,** 960 (1980).
13. P. K. Pal and S. K. De, *Rubber Chem. Technol.*, **55,** 1370 (1982).
14. P. K. Pal, S. N. Chakravarty, and S. K. De, *J. Appl. Polym. Sci.*, **28,** 659 (1983).
15. P. K. Pal and S. K. De, *Rubber Chem. Technol.*, to appear.

Received March 14, 1983
Accepted June 20, 1983